Engineering microphysiological systems for investigating airborne infectious diseases

Bárbara F. Fonseca[1], Jérôme Wong-Ng[1], Michael Connor[2], Héloïse Mary[1], Min Hee Kim[1], Rémy Yim[1], Lisa A. Chakrabarti[3], Samy Gobaa[1]

[1]Institut Pasteur, Université Paris Cité, Biomaterials and Microfluidics core facility, C2RT, Paris, France. [2]Institut Pasteur, Université Paris Cité, Chromatin and Infection laboratory, Paris, France. [3]Institut Pasteur, Université Paris Cité, Control of Chronic Viral Infections Group, Virus and Immunity Unit, Paris, France.

Development of lung organoid on-chip models

Towards functional organotypic models of the respiratory tract epithelia

The development of complex in vitro models, such as organoids, gastruloids and organ-on-chips systems, allow a better understanding of human biological processes that are otherwise difficult to address with classical in vitro 2D culture and/or with animal models. Elucidating how pathogens invade human cells by evading the immune system and how this could be modulated by the host microbiota has been greatly facilitated by the advancement of 3D cell culture techniques.

Our Team is working on establishing unique advanced microphysiological systems that can mimic the interaction between human epithelial barriers with the surrounding tissues, such as blood vessels, mesenchyme and immune cells. We relay both on the use of organoids derived from human tissues and microfluidic chips (Figure 1).

Human lung organoids can give rise to alveolar and airway cell types in organoids and organ-on-chips

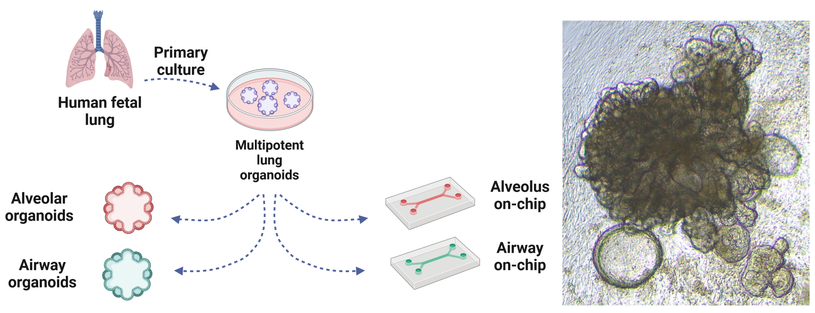

Figure 1: Left: Schematic representation of the cell culture steps to produce different fetal lung organoid types and organ-on-chip devices. Primary fetal lung bud tips are extracted and cultured in 3D in self-renewal conditions. Undifferentiated organoids are expanded in vitro prior to further induction of alveolar and airway differentiation, either in organoids or organ-on-chips. Right: A representative brightfield image of multipotent lung organoids in culture.

Generation of airway and alveolar organoids derived from human fetal lung cells

Producing functional lung-on-chip models relies on the sustainable production of all the cell types populating the respiratory tract. Here, we use primary lung epithelial cells, obtained from fetal samples derived from various gestacional ages (15-24 pcw). Culturing those cells as organoids, in a self-renewal medium, allows the proliferation and maintenance of the multipotent pool of lung epithelial cells (Figure 2). By changing medium composition, we can efficiently induce the differentiation of those lung undifferentiated cells into either alveolar (Figure 3) or airway cells (Figure 4).

Multipotent organoids

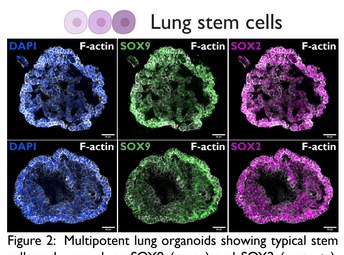

Figure 2: Multipotent lung organoids showing typical stem cell markers such as SOX9 (green) and SOX2 (magenta). Scale bars: 50um.

Alveolar organoids

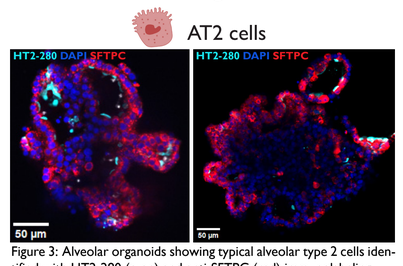

Figure 3: Alveolar organoids showing typical alveolar type 2 cells identified with HT2-280 (cyan) and anti-SFTPC (red) immunolabeling.

Airway organoids

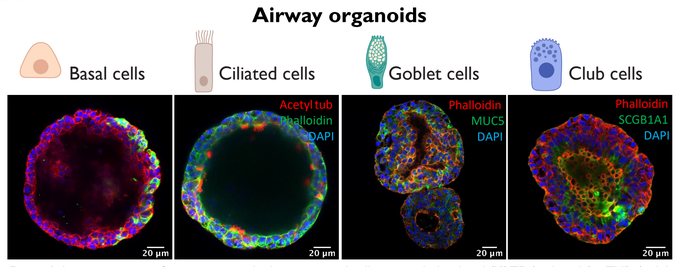

Figure 4: Immunostaining of airway organoids showing typical cell types including basal (KRT5+), ciliated (ac-TUB+), club (SCGB1a1+) and goblet (MUC5AC+) cells.

Characterization of human airway and alveolar organ on-chips

For chip production, we gently dissociate fetal lung organoids and seed them into the top channel of a S1 chip (emulate™). The self-renewal medium is replaced with a differentiation-inducing medium for either airway or alveolar lineages. Primary lung mesenchyme is added in the bottom channel to improve the differentiation status. After epithelial confluency, an air-liquid interface is established and chips are cultured for approximately two and three weeks for alveolar and airway differentiation, respectively (Figure 5-7).

Figure 5: Schematic representation of the protocol used to derive alveolar and airway organoid-on-chip devices.

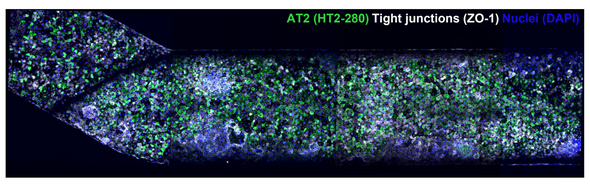

Figure 6: Representative image of the entire chip surface of an alveolar chip showing the tight epithelium (identified by ZO-1 staining) and the presence of alveolar cells (HT2-280+).

Identification of lung cell types on-chip

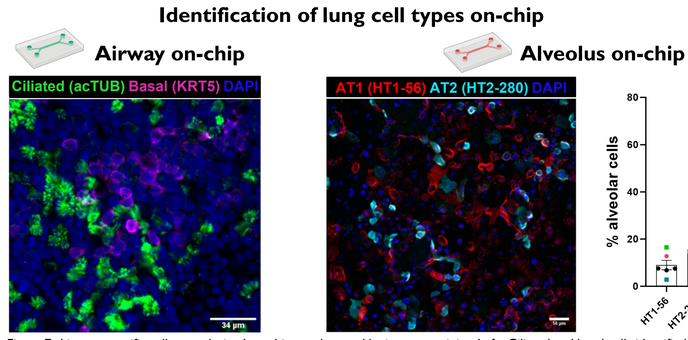

Figure 7: Lineage specific cell types derived on-chip are detected by immunostaining. Left: Ciliated and basal cells identified on airway chips after 21 days of culture. Middle: AT1 and AT2 cells detected on alveolar chips after 14 days culture. Right: Percentage of identified alveolar cells on chip. Each color dot is a different organoid line.

Streptococcus pneumoniae strains infect human alveoli on-chips

Mimicking pneumococcal infections in alveolar chips

Lung organoids cultured on organ-on-chip devices form a tight and polarized epithelium. This provides an easy access to the apical surface of airway and alveolar cells, which is typically targeted by many pollutants and microorganisms in vivo.
To test the feasibility of our lung on chip model to reproduce known pulmonary infections, we exposed lung alveolar cells to *Streptococcus pneumoniae (S. pneumoniae)*. This bacterium is recognized for causing harmful effects in the alveolar surface that rapidly leads to pneumonia (Bogaert et al., Lancet Infect Dis, 2004). For comparison, we used *Corynebacterium accolens* (*C. accolens*), a commensal nasal microbiont that does not colonize the lungs (Bomar et al. mBio, 2016) (Figure 8).

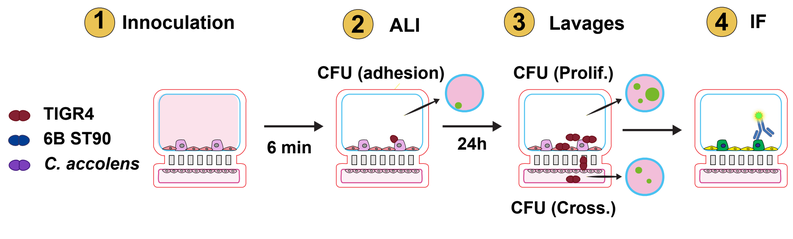

Figure 8: Schematic representation of the infection protocol with *S. pneumoniae* strains (TIGR4 and 6B ST90) or *C. accolens* (commensal control). ALI: air-liquid-interface, IF: immunofluorescence

S. pneumoniae growth on-chips

S. pneumoniae strains (TIGR4 and 6B ST90) rapidly colonize the epithelial surface of lung alveolus on chip (Figure 9). TIGR4, a more agressive strain in vivo (Connor et al. Nature Microbiology, 2021), have increased capacity to cross the epithelial barrier (Figure 9 and 10).

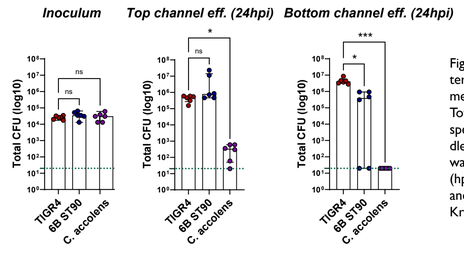

Figure 9: Total CFU counts of bacteria input used for chip experiments (left).
Total CFU counts of bacteria specimens collected in top (middle) and bottom (right) channel washes after 24h post-infection (hpi). Median +/- IQR are plotted and significances compared with Kruskal-Wallys test

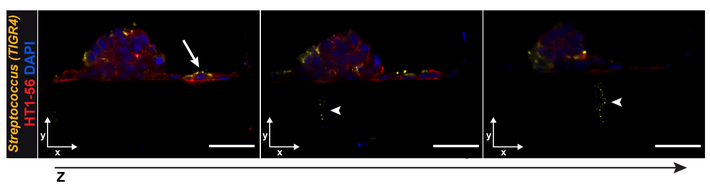

Figure 10: Streptococcus immunolabeling of bacteria specimens surrounding the bottom channel at 24 hours postinfection (hpi). Scale bars: 100 µm

Alveolar cells are susceptible to *S. pneumoniae* colonization

Beyond colonization at 24h post-infection, *S. pneumoniae* cause a deleterious effect in the number of HT2-280+ alveolar cells (Figures 11 and 12). This decrease seems to be specific to this population as no variation in HT1-56+ ATI cells or total cell numbers were observed after TIGR4 or 6B ST90 inoculation.

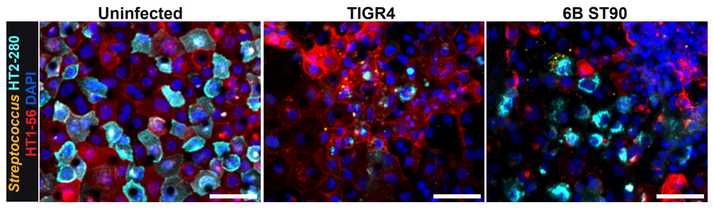

Figure 11: Representative images of bacterium infection in alveolar chips. Scale bar: 50µM

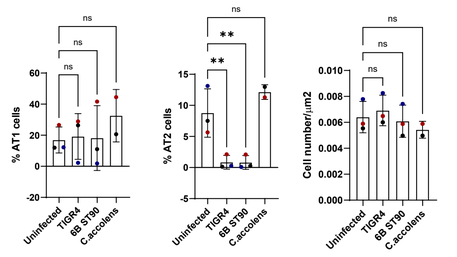

Figure 12: Percentages of AT1 (left) and AT2 (middle) cells upon bacterial infections on-chip. Right: Quantification of number of cells per chip based on the ratio of nuclei number per um² chip area. Means +/- standard deviations are plotted and statistically significant differences compared with one-way ANOVA test. Each dot color represents a different organoid line.

Alveoli on-chip system recapitulates SARS-CoV-2 variant-specific effects

Mimicking SARS-CoV-2 infections in alveolar chips

The COVID-19 pandemic showcased the continuous emergence of novel variants of concern, each using different mechanisms for viral spread and immune evasion to increase infectivity within the respiratory tract. Notably, Omicron sublineages generally replicate faster and more efficiently in the upper respiratory tract epithelium compared to earlier variants. In contrast, in the alveolar microenvironment, Omicron replicates less efficiently than earlier variants such as Delta (Hui et al. Nature 2022). Despite these observations, the mechanisms underlying SARS-CoV-2 variant-dependent tropism remain unclear. To adress this, we employed our alveolar on-chip model to investigate the replication fitness of Delta versus Omicron BA.5 SARS-CoV-2 variants (Figure 13).

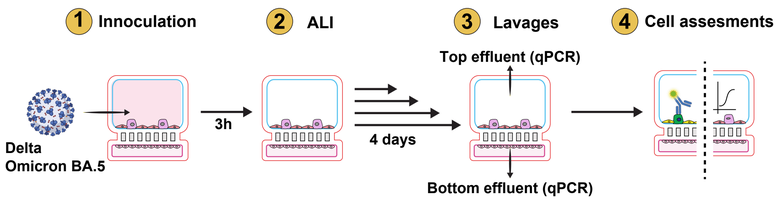

Figure 13: Schematic representation of SARS-CoV-2 infection protocol in alveoli-on-chip system. ALI: air-liquid-interface

SARS-CoV-2 variant Delta infects alveolar type 2 cells

To investigate the replication competence of SARS-CoV-2 virus, we infected alveolar chips with the SARS-CoV-2 Delta variant and chips were then analyzed at 4 days post infection. Immunostaining analyses revealed many SARS-CoV-2 infected cells (stained for spike viral proteins). Approximately one third of infected cells were also positive for AT2 markers such as HT2-280+ or SFTPC (Figure 14).

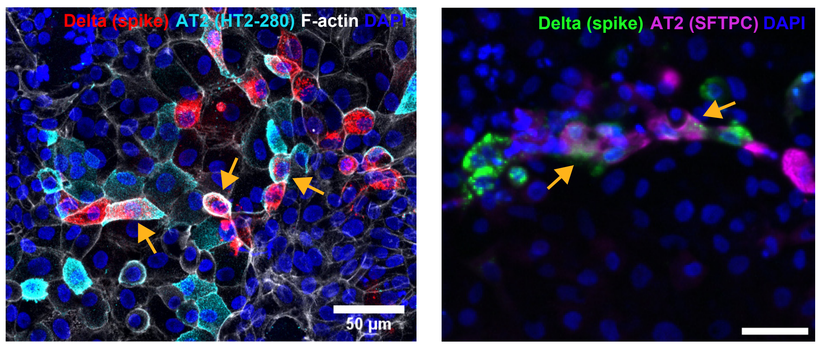

Figure 14: Representative immunostaining images of SARS-CoV-2 (Delta) infection in alveolar chips. Arrows: Infected AT2 cells are identified with HT2-280 and anti-spike antibodies (left) and with anti-SFTPC and anti-spike antibodies (right). Scale bars: 50µM

SARS-CoV-2 variant Delta, but not Omicron BA.5, replicates in human alveolar chips.

To compare SARS-CoV-2 variant fitness, we infected chips with SARS-CoV-2 Delta or Omicron BA.5 variants and quantified apical viral RNA release over 4 days. RT-qPCR data showed a steady Delta replication while Omicron BA.5 did not efficiently replicate in this model (Figure 15). Furthermore, we observed a significant up-regulation of type I Interferon (IFN) pathway, initiating an innate immune response after infection. Interestingly, even with lower replication competence, Omicron BA.5 still triggered a strong epithelial IFN response (Figure 16).

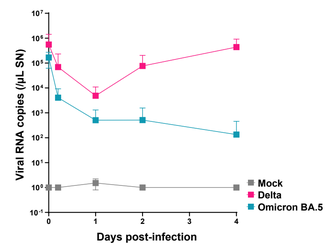

Figure 15: Kinetics of SARS-CoV-2 viral load in top channel effluents measured by RT-qPCR. Mean +/- SD are plotted.

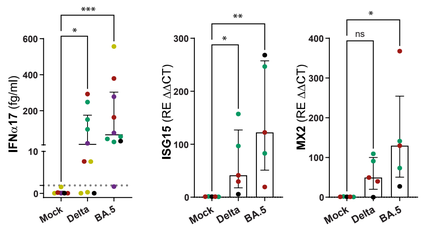

Figure 16: Host IFN response after SARS-CoV-2 infection. Left: IFNα17 proteins detected in top channel washes at 4 dpi. Middle and right: Relative RNA expression of ISG15 and MX2 detected by RT-qPCR at 4dpi. Each dot color represents an organoid line. Median +/- IQR are plotted and Kruskal-Wallis tests used.

Check the preprint!

Acknowledgements: We express our gratitude to H.Strick-Marchand and J. Di Santo for the invaluable support with the fetal lung primary culture; Florence Guivel-Benhassine and Olivier Schwartz for SARS-CoV-2 viruses. This work has been funded in part through a grant from the Covid-19 task force project (Institut Pasteur). We also acknowledge the financial support from Institut Carnot and SPAIS.

Contact:
bdefaria@pasteur.fr